



HHS Public Access

Author manuscript

Nanomedicine. Author manuscript; available in PMC 2017 October 01.

Published in final edited form as:

Nanomedicine. 2016 October ; 12(7): 1827–1831. doi:10.1016/j.nano.2016.03.004.

AntihypoxamiR Functionalized Gramicidin Lipid Nanoparticles Rescue Against Ischemic Memory Improving Cutaneous Wound Healing

Subhadip Ghatak¹, Jilong Li², Yuk C Chan¹, Surya C Gnyawali¹, Erin Steen¹, Bryant C Yung², Savita Khanna¹, Sashwati Roy¹, Robert J Lee², and Chandan K Sen^{1,*}

¹Center for Regenerative Medicine & Cell-Based Therapies, Department of Surgery, Davis Heart and Lung Research Institute, The Ohio State University Wexner Medical Center, Columbus, OH 43210, U.S.A.

²Division of Pharmaceutics and Pharmaceutical Chemistry, College of Pharmacy, The Ohio State University, Columbus, OH 43210, U.S.A.

Abstract

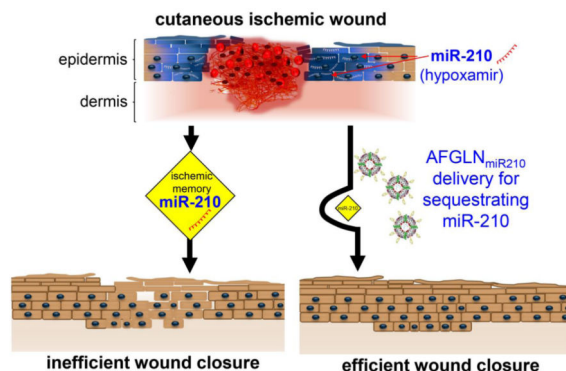
Peripheral vasculopathies cause severe wound hypoxia inducing the hypoxamiR miR-210. High level of miR-210, persisting in wound-edge tissue as ischemic memory, suppresses oxidative metabolism and inhibits cell proliferation necessary for healing. In wound-edge tissue of chronic wound patients, elevated miR-210 was tightly associated with inhibition of epidermal cell proliferation as evident by lowered Ki67 immunoreactivity. To inhibit miR-210 in murine ischemic wound-edge tissue, we report the formulation of antihypoxamiR functionalized gramicidin lipid nanoparticles (AFGLN). A single intradermal delivery of AFGLN encapsulating LNA-conjugated anti-hypoximiR-210 (AFGLN_{miR-210}) lowered miR-210 level in the ischemic wound-edge tissue. In *repTOPTM mitoIRE* mice, AFGLN_{miR-210} rescued keratinocyte proliferation as visualized by *in vivo* imaging system (IVIS). ³¹P NMR studies showed elevated ATP content at the ischemic wound-edge tissue following AFGLN_{miR-210} treatment indicating recovering bioenergetics necessary for healing. Consistently, AFGLN_{miR-210} improved ischemic wound closure. The nanoparticle based approach reported herein is effective for miR-directed wound therapeutics warranting further translational development.

Graphical abstract

* **Corresponding Author:** Chandan K. Sen, Professor & Director, Center for Regenerative Medicine & Cell-Based Therapies, The Ohio State University Wexner Medical Center, 473 West 12th Ave, Columbus, OH 43210. Tel.: 614-247-7658; Fax: 614-247-7818, chandan.sen@osumc.edu.

Publisher's Disclaimer: This is a PDF file of an unedited manuscript that has been accepted for publication. As a service to our customers we are providing this early version of the manuscript. The manuscript will undergo copyediting, typesetting, and review of the resulting proof before it is published in its final citable form. Please note that during the production process errors may be discovered which could affect the content, and all legal disclaimers that apply to the journal pertain.

Disclosure: The authors disclose no conflict of interest.



Successful intervention of non-healing ischemic wound is a major problem. Presence of hypoxia induced miR-210 limits keratinocytes proliferation and compromised wound closure. In this work, we report the formulation of antihypoxamiR functionalized gramicidin lipid nanoparticles (AFGLN). A single intradermal delivery of AFGLN encapsulating LNA-conjugated anti-hypoximiR-210 (AFGLN_{miR-210}) lowered miR-210 level in the ischemic wound-edge tissue. AFGLN_{miR-210} delivery elevated ATP content at the ischemic wound-edge tissue recovering bioenergetics necessary for keratinocyte proliferation. Consistently, AFGLN_{miR-210} improved ischemic wound closure. The nanoparticle based approach reported herein is effective for miR-directed wound therapeutics warranting further translational development.

Keywords

Ischemic wounds; tissue oxygenation; miR-210; keratinocytes proliferation; lipid nanoparticles

Peripheral vasculopathies are primarily responsible for wound ischemia and hypoxia¹. The biological response to ischemia depends largely on the state of hypoxia. If the hypoxia is moderate, allowing for sufficient residual oxygen to support tissue survival, cells minimize oxygen cost by economizing metabolism and makes an effort to mount adaptive solutions. On the other hand, if the hypoxia is severe or near-anoxic, then adaptive rescue is no longer an option. Cells bring down oxygen cost to the threshold that separates survival and death. This is sustainable for a limited time within which the tissue may be rescued by intervention or it yields to necrotic death¹.

Our previous work has recognized the induction of master hypoxamiR miR-210 in keratinocytes of ischemic wound-edge tissue²⁻⁴. Elevated miR-210 lowers oxygen cost of survival by repressing mitochondrial metabolism and attenuating keratinocyte proliferation. miR-210 also silences cell cycle proteins^{2, 3} (Figure S1). Such measures defend survival but oppose healing because tissue repair requires oxidative metabolism and cell proliferation. Although the state of oxygenation of the wound tissue may be corrected by intervention^{1, 5, 6}, growth of wound tissue is limited by an abundance of miR-210 repressing mitochondrial metabolism and cell proliferation. Thus, miR-210 may be viewed as an “ischemic memory” at the wound-edge tissue that is in direct conflict with wound healing. Healing outcomes of such ischemic wound tissue may be maximized by sequestering miR-210. In the present work we report the development of a novel antihypoxamiR

functionalized lipid nanoparticles (LNPs) that is able to rescue against the ischemic memory of miR-210 improving cutaneous wound healing.

Methods

1,2-Dioleoyl-3-dimethylammonium-propane (DODAP), 1,2-dioleoyl-3-trimethylammonium-propane (DOTAP), soy phosphatidylcholine (SPC), gramicidin (GRAM), and d-alpha-tocopheryl polyethylene glycol 1000 succinate (TPGS) were dissolved in ethanol and combined at the molar ratio of 40/5/30/20/5 (DODAP/DOTAP/SPC/GRAM/TPGS). The lipid mixture was then combined with an appropriate amount of LNA based miR-210 power inhibitor in 40% ethanol followed by serial dilution (Appendix A. Supplementary data). Ischemic wound in C57BL/6 and *repTOPTM mitoIRE* mice were induced by creating a bi-pedicle flap². The *repTOPTM mitoIRE* mice express the luciferase reporter gene under the control of an artificial minimal promoter derived from the Cyclin B2 gene, specifically induced during cell proliferation. LNA based anti-miR-210 and negative control were purchased from Exiqon. miRNA isolation, Western blot, immunohistochemistry was performed as describe previously⁷. For further details see supplementary materials.

Results

Laser capture microdissection (LCM) of human ischemic wound-edge epithelium revealed elevated miR-210 expression compared to the non-ischemic epithelium (Figure 1A). Expression of Ki67, a marker of cell proliferation, was also significantly lower in the epithelial tongue⁸ of the human ischemic wound as compared to non-ischemic wound epithelium (Figure 1B). The expression of miR-210 was inversely correlated with the number of proliferating keratinocytes in patients with chronic wounds (Figure 1C). To evaluate the efficacy of anti-miR-210 in ischemic wound closure, a locked nucleic acid (LNA)-based anti-miR-210 power inhibitor (AM-210) was delivered intra-dermally to ischemic wound tissue of mice. At a relatively high dose of 500nM, administration of naked anti-miR-210 was ineffective in neutralizing hypoxia-induced elevated miR-210 in the wound tissue (Figure 1D).

We sought to develop LNPs optimized for the delivery of antagomir cargo to the cutaneous wound tissue. The particle composition and zeta potential were evaluated and presented in Figure 2A & B. The LNPs had an average diameter of 150 nm and a zeta potential of +10 to -10 mV at pH of 5 and 8, respectively. The encapsulation efficiency of these LNPs was found to be 80.12%. This LNP composition was selected for the subsequent experiments and is referred to as antihypoxamir (AM-210) functionalized gramicidin lipid nanoparticles (AFGLN) in this work. The size and concentration of the AFGLN were further examined (NanoSightTM) using nanoparticle tracking analysis (Figure 2C).

Intradermal delivery of AFGLN containing LNA-conjugated AM-210 power-inhibitor (AFGLN_{miR-210}) at the wound-edge tissue in the murine model of ischemic wound significantly limited abundance of hypoxia-inducible miR-210 (Figure 3A). To evaluate the functional effect of AFGLN_{miR-210} on ischemic wound closure, bi-pedicle flaps were

created on C57BL/6mice. Digital planimetry demonstrated significant improvement of closure in AFGLN_{miR-210} group from day 3 post-wounding (Figure 3B). To study whether delivery of AFGLN_{miR-210} accelerated wound re-epithelialization, frozen ischemic wound-edge tissue sections at day 7 post-wounding were stained for keratin-14. Wound re-epithelialization was severely compromised in the ischemic wounds that were treated with empty GLN (devoid of any cargo) alone or AFGLN packed with scrambled oligos (AFGLN_{scramble}) (Figure 3C&D). In contrast, AFGLN_{miR-210} treated ischemic wound showed improved re-epithelialization with the presence of characteristic hyperproliferative epithelium as would be expected in healing wounds (Figure 3D). Because mouse is a loose skin animal and wound contraction may confound closure, we used a splinted wound model to limit contraction. AFGLN_{miR-210} treatment improved re-epithelialization (Figure S2).

Consistent with the above-mentioned favorable effects of AFGLN_{miR-210}, bi-pedicle flaps were created with ischemic wounds on *repTOPTM mitoIRE* mice. As shown in Figure 4A, in a setting where the perfusion of ischemic wound was equally limited in all groups, delivery of AFGLN_{miR-210} rescued cell proliferation (Figure 4B). This finding was substantiated by immunohistochemical detection of Ki67 (Figure 4C). ³¹P NMR studies validated the rescue by demonstrating elevated ATP content at the ischemic wound-edge tissue in AFGLN_{miR-210} treated group compared to GLN alone or AFGLN_{scramble} group (Figure 4D). These observations demonstrate that AFGLN_{miR-210} is effective in restoring oxidative metabolism in ischemic wound edge tissue.

Discussion

Clinical intervention to reoxygenate chronic ischemic wounds such as oxygen therapy, debridement, or recanalization are likely to face metabolic barriers such as the miR-210 ischemic memory which when abundant in the wound tissue resists tissue growth (Figure S3). Thus, neutralizing such barriers are likely to improve the effectiveness of standard clinical interventions aimed at re-oxygenating the ischemic wound tissue. This work offers a lipid nanoparticle-based solution to sequester miR-210 in the wound edge tissue resulting in improved closure of ischemic wounds.

Although liposome-based nanoparticles have been widely used in skin health care, the efficiency of cargo delivery following topical application is questionable^{9, 10}. There is no evidence of lipid nanoparticle based intervention of miR delivery or inhibition in the skin. In cutaneous injury, an additional challenge is the rapid removal of such nanoparticles by wound associated phagocytes¹¹. Furthermore, the wound microenvironment features low pH which influences the dynamics of cargo release to the site of injury¹². Thus design of lipid nanoparticles for skin health application, including tissue repair, must troubleshoot these challenges. Soy phosphatidylcholine has been utilized for the bilayer formation along with cationic lipid with tertiary (DODAP) and quaternary (DOTAP) amine headgroups. Incorporation of Gramicidin A was aimed at improving endosomal escape and facilitating ion channel formation in the lipid bilayer¹³. Intradermal injection of AFGLN was effective in cargo-delivery. Observations of this work substantiate the ischemic memory hypothesis by rescuing wound-re-epithelialization in response to inhibition of hypoxamir miR-210⁴. AFGLN was effective in rescuing the ischemia affected wound tissue and resuming re-

epithelialization. The formulation of AFGLN reported in this work would be effective to deliver any cargo of interest to the healing cutaneous wound tissue. A clear translational advantage of AFGLN is that all material used for its formulation has prior history of FDA approval for human use¹⁴⁻¹⁶.

Supplementary Material

Refer to Web version on PubMed Central for supplementary material.

Acknowledgments

Grant Support: This study was supported by NIH RO1 GM-069589, GM-077185, GM108014 and NINR NR013898, NR015676 to CKS

References

- [1]. Sen CK. Wound Healing Essentials: Let There Be Oxygen. *Wound Repair Regen.* 2009; 17:1–18. [PubMed: 19152646]
- [2]. Biswas S, Roy S, Banerjee J, Hussain SR, Khanna S, Meenakshisundaram G, Kuppusamy P, Friedman A, Sen CK. Hypoxia inducible microRNA 210 attenuates keratinocyte proliferation and impairs closure in a murine model of ischemic wounds. *Proc Natl Acad Sci U S A.* 2010; 107:6976–81. [PubMed: 20308562]
- [3]. Chan YC, Banerjee J, Choi SY, Sen CK. miR-210: the master hypoxamir. *Microcirculation.* 2012; 19:215–23. [PubMed: 22171547]
- [4]. Sen CK, Roy S. OxymiRs in cutaneous development, wound repair and regeneration. *Semin Cell Dev Biol.* 2012; 23:971–80. [PubMed: 23063665]
- [5]. Woo, KY. Assessing chronic wound perfusion in the lower extremity: current and emerging approaches. 2015.
- [6]. Sen CK, Roy S. Oxygenation State as a Driver of Myofibroblast Differentiation and Wound Contraction: Hypoxia Impairs Wound Closure. *J Invest Dermatol.* 2010; 130:2701–3. [PubMed: 21068734]
- [7]. Ghatak S, Chan YC, Khanna S, Banerjee J, Weist J, Roy S, Sen CK. Barrier Function of the Repaired Skin Is Disrupted Following Arrest of Dicer in Keratinocytes. *Mol Ther.* 2015
- [8]. Underwood RA, Carter WG, Usui ML, Olerud JE. Ultrastructural localization of integrin subunits beta4 and alpha3 within the migrating epithelial tongue of in vivo human wounds. *J Histochem Cytochem.* 2009; 57:123–42. [PubMed: 18824633]
- [9]. Campbell CS, Contreras-Rojas LR, Delgado-Charro MB, Guy RH. Objective assessment of nanoparticle disposition in mammalian skin after topical exposure. *J Control Release.* 2012; 162:201–7. [PubMed: 22732479]
- [10]. Watkinson AC, Bunge AL, Hadgraft J, Lane ME. Nanoparticles do not penetrate human skin--a theoretical perspective. *Pharmaceutical research.* 2013; 30:1943–6. [PubMed: 23722409]
- [11]. Nie S. Understanding and overcoming major barriers in cancer nanomedicine. *Nanomedicine (London, England).* 2010; 5:523–8.
- [12]. Mura S, Nicolas J, Couvreur P. Stimuli-responsive nanocarriers for drug delivery. *Nat Mater.* 2013; 12:991–1003. [PubMed: 24150417]
- [13]. Zhang M, Zhou X, Wang B, Yung BC, Lee LJ, Ghoshal K, Lee RJ. Lactosylated gramicidin-based lipid nanoparticles (Lac-GLN) for targeted delivery of anti-miR-155 to hepatocellular carcinoma. *J Control Release.* 2013; 168:251–61. [PubMed: 23567045]
- [14]. Porteous DJ, Dorin JR, McLachlan G, Davidson-Smith H, Davidson H, Stevenson BJ, Carothers AD, Wallace WA, Moralee S, Hoenes C, Kallmeyer G, Michaelis U, Naujoks K, Ho LP, Samways JM, Imrie M, Greening AP, Innes JA. Evidence for safety and efficacy of DOTAP cationic liposome mediated CFTR gene transfer to the nasal epithelium of patients with cystic fibrosis. *Gene therapy.* 1997; 4:210–8. [PubMed: 9135734]

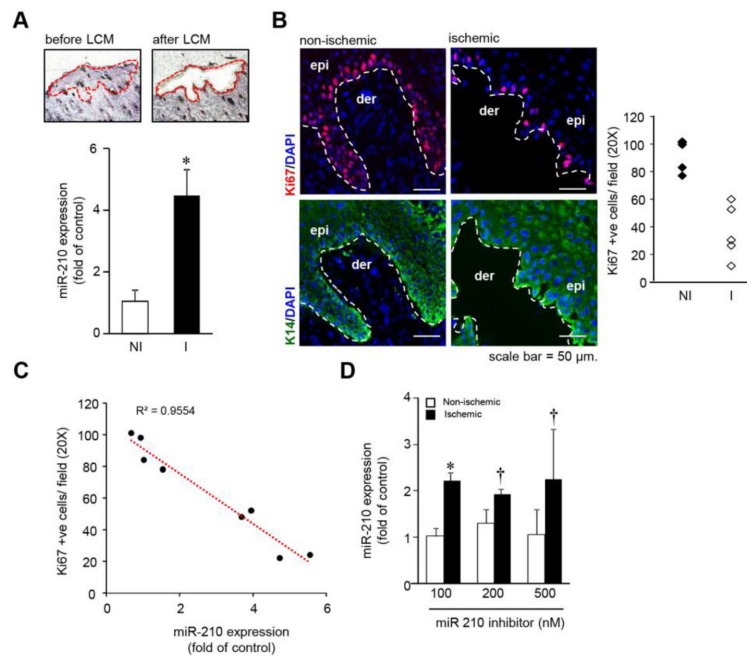
- [15]. Chang H-I, Yeh M-K. Clinical development of liposome-based drugs: formulation, characterization, and therapeutic efficacy. *International Journal of Nanomedicine*. 2012; 7:49–60. [PubMed: 22275822]
- [16]. Guo Y, Luo J, Tan S, Otieno BO, Zhang Z. The applications of Vitamin E TPGS in drug delivery. *European journal of pharmaceutical sciences : official journal of the European Federation for Pharmaceutical Sciences*. 2013; 49:175–86. [PubMed: 23485439]

Author Manuscript

Author Manuscript

Author Manuscript

Author Manuscript

**Figure 1.**

(A) *miR-210* expression from laser microdissected epidermis of human wound-edge tissue. (n=7), * $p < 0.001$; ANOVA. (B) Serial human wound cross-sections stained with anti-Ki67 and keratin-14 antibody, counter stained with DAPI. (n=4-5). The plot represents quantification of the Ki67 positive cells/ field (20X). (C) Regression plot of *miR-210* expression from the human wound edge biopsies against number of Ki67 positive cells/ field (20X). (n=8) (D) *miR-210* expression from murine non-ischemic and ischemic wound-edge tissue 24h after intradermal delivery of naked LNA-anti-*miR-210*. (n=4). * $p < 0.01$; † $p < 0.05$ compared to nonischemic wound, ANOVA.

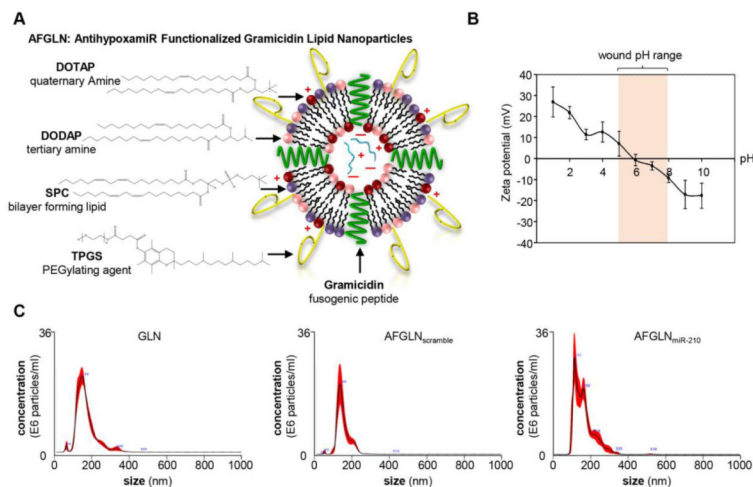


Figure 2. (A) Schematic representation of the AntihypoxamiR Functionalized Gramicidin Lipid Nanoparticles (AFGLN). (B) The zeta potential of the AFGLN at different pH. Shaded region represents the pH range in chronic wounds. (C) Representative nanoparticle tracking analysis (NanoSight™) showing particles size and concentration of the empty GLN (devoid of any cargo), AFGLN packed with scrambled oligos (AFGLN_{scramble}) and AFGLN packed with anti-miR-210 (AFGLN_{miR-210}) (n=4).

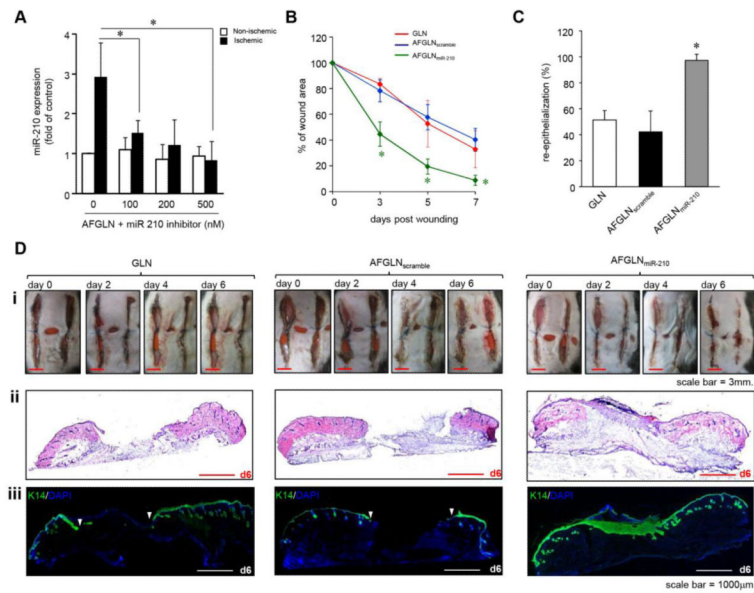


Figure 3. (A) *miR-210* expression from murine non-ischemic and ischemic wound-edge tissue 24h after intradermal delivery of AFGLN_{miR-210}. (n=4). * $p < 0.01$ compared to AFGLN, ANOVA. (B) Wound closure after delivery of empty GLN, AFGLN_{scramble} and AFGLN_{miR-210}. (n=5), * $p < 0.001$ compared to d0; ANOVA. (C) The percentage of re-epithelialization at day 6 post wounding was plotted graphically. (n=3), * $p < 0.001$; ANOVA. (D) (i) Digital photographs of murine ischemic wound at days 0, 2, 4 and 6 after delivery of empty GLN, AFGLN_{scramble} and AFGLN_{miR-210}. (ii) H&E images stained sections from ischemic wounds at day 6 post-wounding. (iii) Wound cross sections were stained with anti-keratin 14 antibody and counterstained with DAPI to show re-epithelialization at day 6 following treatment with GLN, AFGLN_{scramble} and AFGLN_{miR-210}. (n=4).

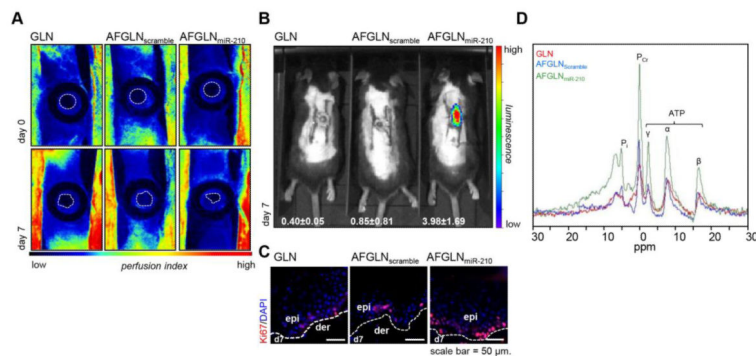


Figure 4.

(A) Laser speckle image showing perfusion level in the bi-pedicle flap at day 0 and day 7 after delivery of only GLN, AFGLN_{scramble} and AFGLN_{miR-210} (B) IVIS image from *repTOP*TM *mitoIRE* showing cell proliferation in animal treated with lipid nanoparticles with AFGLN_{miR-210}. The images from quantification of the mean luminescence has been presented. (n=3) (C) Serial wound cross-sections stained with anti-Ki67 antibody counter stained with DAPI (blue). (n=3). (D) ³¹P NMR spectra of the ischemic wound-edge tissue at day 7 post wounding showing iP, and the three subunits α-, β- and γ- subunit of ATP normalized with phosphocreatinine.